Chapter 13

The Fifth Coming Of Vortices

In 1993 I discovered a unique spacetime spiral element called the *toryx*. The ability of the toryx to be turned inside out made it perfect for modeling polarized prime elements of matter. At about the same time I discovered a close offspring of the toryx called the *helyx* that appeared to be ideal for modeling polarized prime elements of radiation particles. These two discoveries led me to the development of a new version of the vortex theory called *Three-Dimensional Spiral String Theory* (3D-SST).

As any new theory, 3D-SST includes several ideas that some scientists may find controversial. To avoid any confusion, the author separated the parts of theory that are based on prudent conventional assumptions from the parts that required some speculative propositions. Following this approach, this chapter describes a stand-alone spacetime model of toryx and helyx. The model is based on several clear non-speculative assumptions, and its equations can readily be verified by using commonly known mathematical methods. Chapters 14 and 15 outline some possible applications of the spacetime model for defining main properties of prime elements of the universe and their offspring, the particles of ordinary matter described by the conventional physics, and also the exotic particles of dark matter and dark energy.

Chapter 16 outlines a possible way of unification of strong, superstrong (color), gravitational, and electric forces. Here again the proposed theory is divided in two parts. The first part describes in pure mathematical non-speculative terms the Coulomb forces between thin rings with evenly distributed electric charges. Then the second part utilizes the above mathematical model to explain strong, superstrong (color) and gravitational forces between particles.

The Universal Helicola

In 1992, I knew nothing about the existence of the vortex theory. It all started in December of that year during a dinner conversation with my son Gene, who was finishing his last year of high school. Although, besides high school, I studied physics thoroughly while doing both M.S. and Ph.D degrees, none of my professors had ever mentioned this theory,

and I did not remember any references to this subject in the textbooks available to me. For some reason Gene was briefly in a philosophical mood during that fateful evening, and while looking at a crumb of bread, he made a casual observation: "There is probably another world inside that piece."

Even though I heard this notion more than once before, somehow it registered in my mind differently this time. So, I tend to agree with Gene and with all the other people who believe that there is a world that looks like a small pinhead to us and also that our world may look like a pinhead to beings of a much larger world than ours. It was, however, one thing to agree with the exciting idea of a multiple-level universe and a completely different thing to envision it. Intuitively, I thought that the solution of this problem could be found in geometry. It turned out to be a right direction for my search. After a few sleepless nights and almost uninterrupted thinking during a vacation with my wife at a beautiful resort in Phoenix, Arizona, I discovered a geometrical shape that would perfectly represent the infinitude of the world and its repetitious character in both enlarging and diminishing directions. This shape was the endless multiple-level spiral that I named *helicola.* Impressed by its beauty and simplicity along with its unique properties, I became convinced that the helicola certainly deserves to be called the "spiral of the spirals."

But is the helicola merely a product of my abstract imagination? A few days later, after looking at the beautiful blue Arizona sky, I realized that helicola was present in nature since the beginning of time. Moreover, it must be at the core of the universe. You may rightfully be puzzled by my discovery. The astronomers have been scanning the skies for many centuries. The Hubble Telescope had recently provided us with spectacular views of previously unseen galaxies and with unimaginable extraterrestrial formations located many billions of light years away from us. But, besides confirming the already known fact that many galaxies are spiral, nobody had found yet any presence of spiral shape in other celestial structures. Is it really there? Of course, it is.

There is a simple explanation why, in spite of a great resolution of contemporary telescopes, we failed to detect the spiral nature of the universe in the instant images of visible matter:

> *The hidden spiral nature of the universe will immediately become visible as soon as we begin looking not at the matter, but at the way it moves in space.*

Please join me in the exciting venture of discovering the spiral nature of the universe. In the course of this venture, we are not going to use any telescopes; neither will we use a yoga technique employed by Leadbeater and Besant. Instead, we will utilize available astronomical data assisted

by our common sense. Let us begin from asking a simple question: "What is the path of the Earth in space?" Most people whom I asked this question had promptly responded that this path is *elliptical*. Some of them even referred to the Kepler's Laws to support their answer. Well, although many students may still get an A in school for giving this answer, but, as you will see in a moment, this answer does not describe a true trajectory of our planet. Unfortunately, many of our teachers failed to mention to us the fact that Kepler derived his laws when the Sun was believed to be the center of the universe. It was a revolutionary idea during his times, but certainly not now when we know that the Sun is merely one of the stars moving around the center of our galaxy, Milky Way, and that our galaxy is also moving in space.

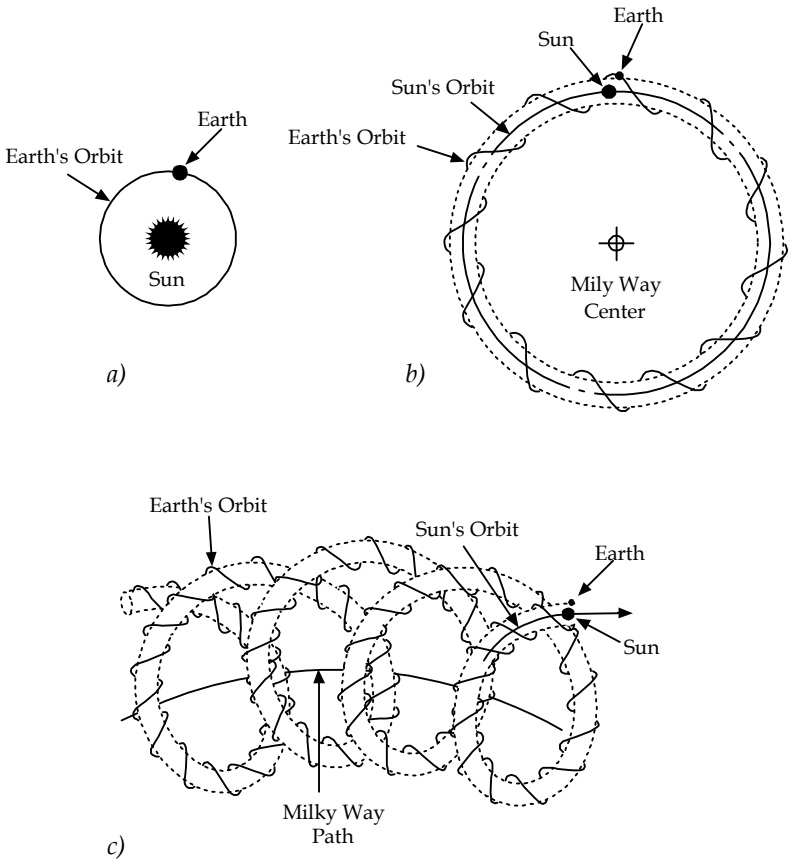

Fig. 13.1. Appearances of the Earth's path in space.

Thus, the appearance of the Earth's path in space depends on a position of an observer. The observer located above the center of the Sun

will see the Earth moving along its elliptical path around the Sun (Fig. 13.1a) at the average velocity of 29.79 km/s, exactly as we were taught in school. However, the appearance of the Earth's trajectory will immediately change as soon as the observer relocates to a place distant from the Sun. Since the Sun moves around the center of our galaxy, the Milky Way, at the average velocity of about 240 km/s, the observer located above the center of our galaxy will see the Earth's path as a helical spiral wound around the Sun's path (Fig. 13.1b).

Is this a final "world line" for our planet? No, it is not. According to the latest astronomical data, our galaxy rushes towards the constellation Hydra at velocity of 600 km/s. So, to an observer located far away from the path of the Milky Way, the Earth's path will look like a dual-level spiral in which one helical spiral is wound around another helical spiral (Fig. 13.1c). Nowadays we know nothing about a gigantic mysterious object around which the Milky Way moves. But an observer located far away from the gigantic mysterious object would see the Earth's path as a triple-level helical spiral. To an observer located at an even greater distance from the Earth, the "world line" of our planet will look as a quadruple-level helical spiral, and so on and so on. This multiple-level helical spiral is helicola. Thus,

> Helicola is a multiple-level spiral in which a helical spiral of a certain level is wound around a spiral path of a helical spiral of an adjacent lower level.

We are not just passive observers of helicola, but its intimate companions. Each of us is traveling in space continuously along an individual helicolical path. The precise "world line" of each person depends on his or her location. For instance, those of us who are located at the altitude of New York will advance every one hour about 1200 km along the level n of helicola that coincides with the trajectory of the rotation of the Earth's surface around its axis. During the same time, we will advance about 107,240 km along the level $(n - 1)$ of helicola that coincides with the orbital path of the Earth around the Sun. In addition, during the same one hour we will advance about 864,000 km along the level $(n - 2)$ of helicola that is the orbital path of the Sun around the center of galaxy. The next level $(n - 3)$ of helicola coincides with the trajectory of the center of our galaxy in its journey towards the constellation Hydra. This motion will add another whooping 2,160,000 km to our travel distance covered during the same one hour. But, the constellation Hydra is not standing still either. So, during the same hour, we may have also advanced many millions of kilometers along the level $(n - 4)$ of helicola, also along the levels $(n - 5)$, $(n - 6)$, and so on and so on.

Our path in space is certainly different from the one impressed in our minds from learning about Kepler's elliptical orbits and the galaxies flying apart after the Big Bang. To the delight of some scholars who avoid discussing new ideas that are not widely accepted by the scientific community, the discovery of helicola required neither a help from any speculative propositions nor a use of any unproven astronomical data. All the facts were available long ago, and I was able to discover the celestial helicola only by looking at the same data from a different angle.

Soon after our return back home from Phoenix, in 1993, I wrote a short essay "Multiple-Level Universe" and sent a few copies to several scientists in the United States. Among the received responses the most encouraging was from Dr. Carlo Rovelli then of the University of Pittsburgh who described my little essay as "delightful and stimulating." This marked a beginning of my serious research on spirals that still continues without any interruption. One of the first questions that bothered me the most was: "What is the origin of the spiral motion in the universe?" The more I read about the vortex theory the more I tended to agree with some developers of this theory that the origin of the spiral motion in the universe is hidden in the dynamics of its internal structure that goes all the way down to the *prime elements of matter and energy*.

CONSTRUCTION OF TORYX

I began my research on spirals from finding an abstract mathematical model for a simplest version of helicola. I chose a geometrical shape that had only two levels of helicola, the minimum number of levels for the spiral to be qualified as helicola. You can easily follow the construction of this shape. Consider two points, m and n in Figure 13.2. Both points are separated from each other by 180 degrees and rotate around a point O at the rotational velocity V_{1r}. These points create two circular traces A_1 with radius r_1 called the *toryx leading string*. The points m and n serve as pivots for the points a and b separated from each other by 180 degrees and moving along a circle with radius r_2. Rotational velocities of the points a are indicated as V_{2r}. Thus, each point a is involved in two motions: a translational motion together with the points m and n at the translational velocity $V_{2t} = V_{1r}$ and a rotational motion around the points m and n at the rotational velocity V_{2r}. The same is true for the point b. The combined motions of the points a and b create two sets of double-toroidal spiral traces A_2 separated from each other by 180 degrees. One set is associated with the pivot point m, while the other one with the pivot point n. The two sets of the double-toroidal spiral traces form the *toryx trailing string* A_2. The radius of the toryx eye r_i is called the *radius*

of real inversion string. Physical meaning of this name will be clear later.

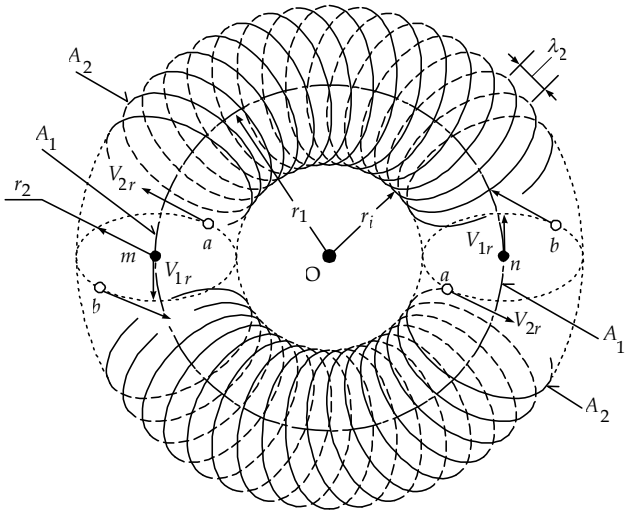

Figure 13.2. Construction of a toryx.

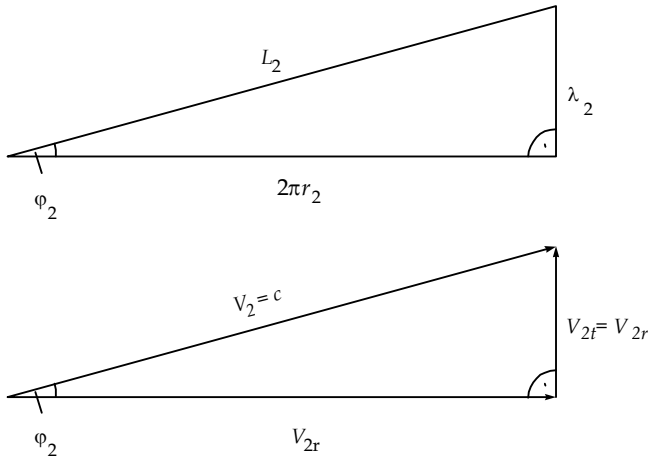

Figure 13.3. Spacetime parameters of a toryx.

One of the most important features of the toryx is a capability of its double toroidal trailing string to propagate along its spiral path in synchrony with the double-circular leading string. The requirement for the synchronization of motions of these strings is met when the rotational velocity of the leading string V_{1r} is equal to the translational velocity of the trailing string V_{2t} ($V_{1r} = V_{2t}$). According to the Pythagorean Theorem

for the right triangle, the spiral velocity of the trailing string V_2 is equal to a geometrical sum of rotational and translational velocities of this string, V_{2r} and V_{2t} (Fig. 13.3).

Besides the parameters mentioned above, the spacetime properties of the toryx can also be described by several other parameters of leading and trailing strings, including the lengths of one winding of the strings L_1 and L_2, the string wavelengths λ_1 and λ_2, the string frequencies f_1 and f_2, the time periods T_1 and T_2, the number of windings w_1 and w_2, and the steepness angles φ_1 and φ_2. Because the leading string is circular, $\lambda_1 = 0$, $w_1 = 1$, and $\varphi_1 = 0$.

SPACETIME PARAMETERS OF TORYX

Let us begin our story from describing the fundamental spacetime equations for the toryx. The purpose of these equations is two-fold. Firstly, they drastically reduce a variety of possible spacetime configurations of the toryces, and secondly, they yield the spacetime properties of the toryx that could readily be associated with physical properties of potential prime elements of nature. The fundamental equations shown in Table 13.1 establish the assumed relationships between the spacetime properties of leading and the trailing strings of the toryx.

Table 13.1. Fundamental spacetime equations for a toryx.

Parameter	Equation	
Radius of real inversion string	$r_i = r_1 - r_2 = const.$	(13-1)
Length of one winding of trailing string	$L_2 = L_1$	(13-2a)
Steepness angle of trailing string	$\cos\varphi_2 = \frac{r_2}{r_1}$	(13-2b)
Spiral velocity of trailing string.	$V_2 = \sqrt{V_{2t}^2 + V_{2r}^2} = c$	(13-3)

To a delight of the lovers of a simple math, the fundamental spacetime equations of a toryx use only basic mathematical functions. The meaning of these equations is very clear. Equation (13-1) states that the difference between the radii of leading and trailing strings r_1 and r_2 is equal to the radius of the real inversion string r_i that is constant. Equation (13-2a) requires the length of one winding of the trailing string L_2 to be equal of that of the leading string L_1. Equation (12-2b) stipulates that, for the middle of trailing string, the cosine of the steepness angle of this

string φ_2 is equal to the ratio of radii of trailing and leading strings r_2 and r_1. It shall be noted that Equations (13-2a) and (13-2b) yield the same spacetime toryx characteristics, and can be used interchangeably.

You may readily recognize in Equation (13-3) a particular case of the Pythagorean Theorem for the right triangle. In application to the toryx this theorem states that the spiral velocity of the trailing string V_2 is equal to the geometrical sum of the translational velocity V_{2t} and the rotational velocitiy V_{2r} of the trailing string. In addition, the spiral velocity of the trailing string V_2 is constant and equal to the *ultimate string velocity c*.

So far, everything is very simple and easy to understand. But, we shall expose some hidden intricacies of the four deceivingly simple fundamental spacetime equations of the toryx:

- Unlike a general view that the radii of a toroidal spiral must be only positive, the radii of both the leading string r_1 and the trailing string r_2 of the toryx can be either positive or negative. But their difference remains equal to a constant positive value of the radius of real inversion string r_i according to Equation (13-1).
- Unlike a general view that the range of cosine of an angle must be within ± 1, the range of cosine of the steepness angle of toryx trailing string φ_2 is unlimited and is within $\pm \infty$.
- Unlike a general view that velocities can only be expressed by real numbers, the translational velocity of the toryx trailing string V_{2t} can also be expressed by imaginary numbers. Consequently, the rotational velocity of the toryx trailing string V_{2r} can be either less or greater than the ultimate string velocity *c*.

Based on the four toryx fundamental equations shown in Table 13.1, one can readily derive the equations describing the spacetime properties of the toryx principal parameters shown in Table 13.2. To make this task easier, we expressed the toryx spacetime parameters in relative terms in respect to the four constant parameters: the radius of real inversion string r_i, the circumference of real inversion string $2\pi r_i$, the ultimate string velocity *c*, and the *frequency of real inversion string* f_i that is equal to:

$$f_i = \frac{c}{2\pi r_i} = const. \qquad (13\text{-}4)$$

The obtained equations allow us to analyze what happens with the toryx parameters as the relative radius of its leading string b_1 changes from $-\infty$ to $+\infty$. Since all the toryx parameters are expressed in relative terms, there is no need to know absolute values of any constants, includ-

ing the radius of real inversion string r_i, the ultimate string velocity c, and the frequency f_i, to perform this analysis.

Table 13.2. Spacetime parameters of a toryx at a middle point.

Parameters	Leading string	Trailing string
Relative string radius	$b_1 = \frac{r_1}{r_i}$	$b_2 = \frac{r_2}{r_i} = b_1 - 1$
Steepness angle	$\varphi_1 = 0$	$\cos\varphi_2 = \frac{b_1 - 1}{b_1}$
Relative wavelength	$\eta_1 = \frac{\lambda_1}{2\pi r_i} = 0$	$\eta_2 = \frac{\lambda_2}{2\pi r_i} = \sqrt{2b_1 - 1}$
Relative length of one string winding	$l_1 = \frac{L_1}{2\pi r_i} = b_1$	$l_2 = \frac{L_2}{2\pi r_i} = b_1$
The number of windings per string	$w_1 = 1$	$w_2 = \frac{b_1}{\sqrt{2b_1 - 1}}$
Relative translational velocity	$\beta_{1t} = \frac{V_{1t}}{c} = 0$	$\beta_{2t} = \frac{V_{2t}}{c} = \frac{\sqrt{2b_1 - 1}}{b_1}$
Relative rotational velocity	$\beta_{1r} = \frac{V_{1r}}{c} = \frac{\sqrt{2b_1 - 1}}{b_1}$	$\beta_{2r} = \frac{V_{2r}}{c} = \frac{b_1 - 1}{b_1}$
Relative spiral velocity	$\beta_1 = \frac{V_1}{c} = \frac{\sqrt{2b_1 - 1}}{b_1}$	$\beta_2 = \frac{V_2}{c} = 1$
Relative frequency	$\delta_1 = \frac{f_1}{f_i} = \frac{\sqrt{2b_1 - 1}}{b_1^2}$	$\delta_2 = \frac{f_2}{f_i} = \frac{1}{b_1}$
Relative time period	$t_1 = T_1 f_i = \frac{b_1^2}{\sqrt{2b_1 - 1}}$	$t_2 = T_2 f_i = b_1$

It is important to keep in mind that the equations listed in Table 13.2 are applicable to the middle point a of the toryx trailing string (Fig. 13.4). But some toryx parameters vary along the spiral path of the trailing string. It is clear from Figure 13.4 that the translational velocity β_{2t} at each point of the trailing string is proportional to the distance from the toryx center. At the same time, the rotational velocity β_{2r} of the trailing string changes in such a way that each point of the trailing string propagates at a constant spiral string velocity equal to the ultimate string velocity c.

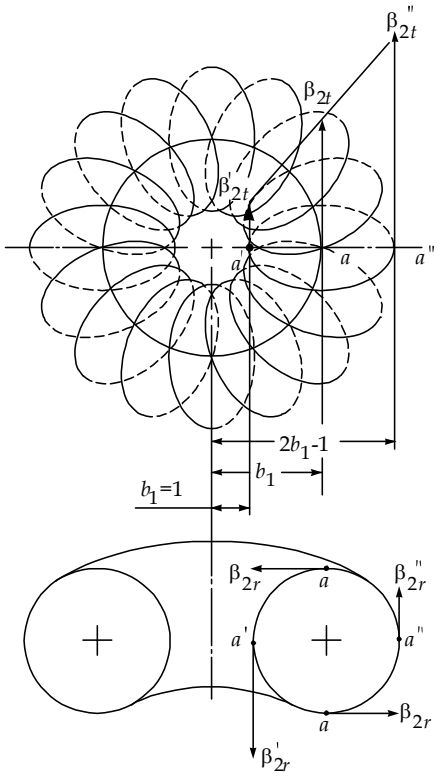

Figure 13.4. Peripheral and middle velocities of the toryx trailing string.

Table 13.3. Relative peripheral and middle velocities of the toryx trailing string.

Points on trailing string (Fig. 13.4)		
Inner point a'	Middle point a	Outer point a''
$\beta'_{2t} = \dfrac{\sqrt{2b_1 - 1}}{b_1^2}$	$\beta_{2t} = \dfrac{\sqrt{2b_1 - 1}}{b_1}$	$\beta''_{2t} = \dfrac{(2b_1 - 1)\sqrt{2b_1 - 1}}{b_1^2}$
$\beta'_{2r} = \dfrac{\sqrt{b_1^4 - 2b_1 + 1}}{b_1^2}$	$\beta_{2r} = \dfrac{b_1 - 1}{b_1}$	$\beta''_{2r} = \dfrac{\sqrt{b_1^4 - (2b_1 - 1)^3}}{b_1^2}$

Table 13.3 shows the equations for the relative peripheral translational velocities (β'_{2t} and β''_{2t}) and the relative peripheral rotational velocities (β'_{2r} and β''_{2r}) of a trailing string. From these equations we find that for some real toryces, the peripheral translational velocity of the trailing string becomes superluminal, while its middle translational velocity remains subluminal. This occurs when the relative radius of the toryx leading string is within the range:

$$0.5437 < b_1 < 6.2223 \qquad (13\text{-}4)$$

INVERSION OF TORYX STRINGS

According to Equations shown in Tables 13.1 and 13.2, the toryx parameters change with the change of the radius of its leading string r_1 (or b_1 in relative terms). During this change the toryx undergoes through a dramatic transformation of its shape that involves inversion of its strings. We discussed the inversion phenomenon in Chapter 7. There is a great chance that you know the meaning of this word. You stumble upon inversion every time you turn your shirt inside out, sometimes by mistake. Some clothes designers even make use of the capability of clothes to be turned inside out and design them two-sided with different colors. The toryx strings can be turned inside out in the same way.

To "visualize" the inversion states of the toryx strings, we presented the strings in the form of ribbons with their opposite surfaces colored in black and white. The inversion state of a string is defined by its external color. A string with the black external color is called *outverted*, or *negative*. Conversely, after the string is turned inside out, its external color becomes white, and it is called *inverted*, or *positive.*

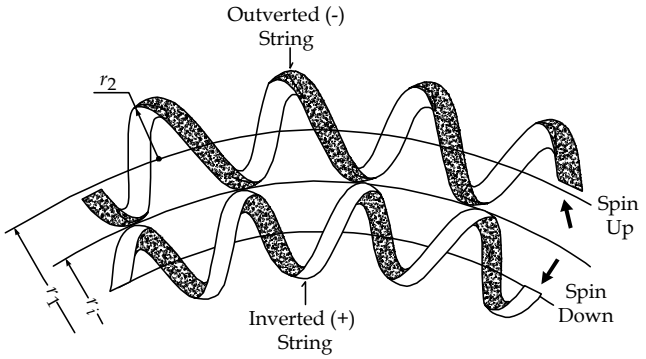

Fig. 13.5. Inversion of the toryx the trailing string.

Let us consider a transformation of a trailing string wound outside the *inversion sphere* with radius r_i (Fig. 13.5). This string is outverted, its radius is positive ($r_2 > 0$), and its external color is black. According to equations shown in Table 13.2, as long as r_1 remains greater than r_i, nothing out-of-ordinary happens when r_1 decreases: the trailing string simply becomes slimmer, and the number of its windings w_2 decreases. But when $r_1 = r_i$, a real transformation of a toryx occurs. Since in that case $r_2 = 0$, the trailing string reduces to a circle with a single winding

(w_2 = 1) that appears in Figure 13.5 as a colorless edge of a ribbon. When $r_1 < r_i$, the sign of its radius r_2 changes from positive to negative; the trailing string turns inside out, or becomes inverted. Consequently, its external color becomes white and its spin reverses. Importantly, the spin of the outverted trailing string can be either *up* (clockwise) or *down* (counter-clockwise). Thus, the spin of the inverted trailing string will be respectively reversed to be either down or up.

The transformation of the toryx leading string proceeds in a similar manner (Fig. 13.6). When radius of the leading string is positive ($r_1 > 0$), it is outverted, so its external color is black. When r_1 = 0, the leading string reduces to a point, making a ribbon both dimensionless and colorless. When r_1 becomes negative ($r_1 < 0$), the leading string turns inside out, or becomes inverted, making its external color white.

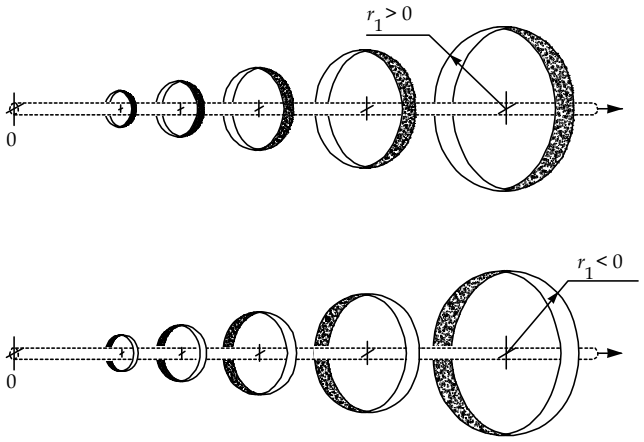

Fig. 13.6. Inversion of the toryx leading string.

For a quantitative description of the inversion state of the entire toryx, we use the so-called *toryx curvature factor q* that is equal to the ratio of the radii of trailing and leading strings r_2 and r_1 with a negative sign:

$$q = -\frac{r_2}{r_1} = -\frac{b_2}{b_1} = -\frac{b_1 - 1}{b_1} \qquad (13\text{-}5)$$

THE AMAZING TRIANGLE OF VELOCITIES

We will use the Pythagorean Theorem very familiar to us to describe the relationships between velocities of the trailing string. But, please do not

be deceived by apparent simplicity of the Pythagorean equation, because we are going to expand its application into the range that is not conventionally used. So, you may need to apply your imagination to visualize some unusual properties of a toryx that make this element unique.

Consider a right triangle representing the relative velocities of the trailing string corresponding to the middle of the string: the rotational velocity β_{2r}, the translational velocity β_{2t}, and the spiral velocity $\beta_2 = 1$. Then from the toryx fundamental spacetime equation (13-3) shown in Table 13.1 we obtain:

$$\beta_{2t}^2 + \beta_{2r}^2 = 1 \tag{13-6}$$

It is important to emphasize again that in the above equation the values of the relative rotational velocity β_{2r} are not restricted, and can range from negative to positive infinity. Consequently, when $\beta_{2r} < 1$, β_{2t} is real, and when $\beta_{2r} > 1$, β_{2t} is imaginary. As shown in Table 13.2, the relative rotational velocity β_{2r} is related to the relative radius of the leading string b_1 and the string steepness angle φ_2 by the equation:

$$\beta_{2r} = \frac{b_1 - 1}{b_1} = \cos\varphi_2 \tag{13-7}$$

Thus, similar to the rotational velocity β_{2r}, the magnitude of $\cos\varphi_2$ can vary from negative to positive infinity.

Let us now consider the evolution of both the rotational velocity β_{2r} and the translational velocity β_{2t} with a change of the steepness angle φ_2 of the trailing string (Fig. 13.7).

Figure 13.7a - When $\varphi_2 = 0$ ($b_1 \to +\infty$), according to Equation (13-7), the rotational velocity $\beta_{2r} = 1$, and the right triangle of velocities reduces to a straight line.

Figure 13.7b - Within the range $0 < \varphi_2 < 90^0$ ($1 < b_1 < +\infty$), the triangle of velocities contains both the rotational velocity β_{2r} and the translational velocity β_{2t}, which magnitudes are expressed with real numbers. If β_{2r} is known, then β_{2t} can readily be calculated from Equation (13-6). For instance, for $\beta_{2r} = 0.99$, we obtain:

$$\beta_{2t} = \sqrt{1 - \beta_{2r}^2} = \sqrt{1 - 0.99^2} = 0.141$$

Figure 13.7c - When $\varphi_2 = 90^0$ ($b_1 = 1$), the triangle of velocities reduces again to a straight line when $\beta_{2t} = 1$ and $\beta_{2r} = 0$. This is a crossover point at which the direction of the rotational velocity β_{2r} changes.

Figure 13.7d - Within the range $90^0 < \varphi_2 < 180^0$ ($\frac{1}{2} < b_1 < 1$), the triangle of velocities contains both β_{2r} and β_{2t}, but the rotational velocity β_{2r} changes its sign.

Figure 13.7e - When $\varphi_2 = 180^0$ ($b_1 = ½$), the right triangle of velocities reduces to a straight line again. This is another crossover point at which $\beta_{2t} = 0$ and $\beta_{2r} = -1$. As long as the string steepness angle φ_2 does not exceed 180^0, there is still nothing unusual in the behavior of the right triangle.

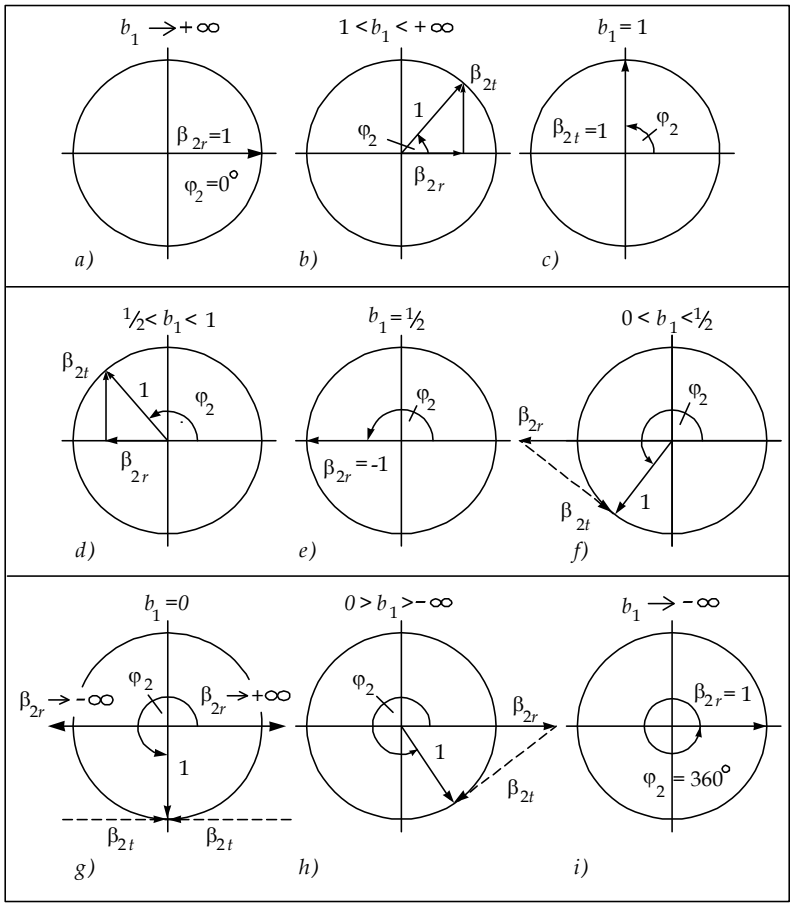

Figure 13.7. Velocity hodographs of the toryx trailing string.

Figure 13.7f - Within the range $180^0 < \varphi_2 < 270^0$ ($0 < b_1 < ½$), we encounter an interesting phenomenon: the rotational velocity of the trailing string exceeds the ultimate string velocity c, so $\beta_{2r} > 1$. Consequently, one side of the triangle of velocities becomes greater than its hypotenuse, and the triangle of velocities inverses. It is easy to see that the triangle of velocities shown in Fig. 13.7f is inverted in respect to that shown in Fig. 13.7d. In the inverted triangle, the rotational velocity β_{2r}

becomes hypotenuse, and the relative ultimate string velocity ($\beta_2 = 1$) converts into one of its legs.

The inversion of the triangle of velocities does not prevent us from using the Pythagorean Theorem for calculation of the translational velocity β_{2t}. For instance, for $\beta_{2r} = 1.01$, we will obtain from Equation (13-6) that the translational velocity β_{2t} is expressed with an imaginary number:

$$\beta_{2t} = \sqrt{1 - \beta_{2r}^2} = \sqrt{1 - 1.01^2} = 0.141i$$

Thus, at $\varphi_2 = 180^0$, a transition takes place from a *real toryx* to an *imaginary toryx*. It is useful to remember that in the real toryx, the rotational velocity of the trailing string V_{2r} is less than the ultimate string velocity ($\beta_{2r} < 1$), while in the imaginary toryx, it is greater than the ultimate string velocity ($\beta_{2r} > 1$). As φ_2 continues to increase, b_1 gets closer to zero, the negative value of β_{2r} increases, and the right triangle of velocities continues to elongate.

Figure 13.7g – At $\varphi_2 = 270^0$ ($b_1 = 0$), we pass through another crossover point at which the direction of the rotational velocity β_{2r} reverses from negative infinity to positive infinity.

Figure 13.7h – Within the range $270^0 < \varphi_2 < 360^0$ ($0 > b_1 > -\infty$), as φ_2 continues to increase, the negative value of b_1 increases, the positive value of β_{2r} decreases, and the right triangle of velocities becomes smaller.

Figure 13.7i – When $\varphi_2 = 360^0$ ($b_1 \rightarrow -\infty$), the right triangle of velocities reduces to a straight line, and the rotational velocity β_{2r} becomes equal to 1. Now, compare Figures 13.7a and 13.7i. They are completely identical in all aspects, except for one important difference. In Figure 13.7a, b_1 approaches positive infinity ($+\infty$), while in Figure 13.7i it approaches negative infinity ($-\infty$). Here you are witnessing a great *phenomenon of merging positive and negative infinities*. This phenomenon, however, is not limited to the relative radii of the leading string b_1. The infinities also merge for several other toryx parameters when $\varphi_2 = 270^0$ ($b_1 = 0$).

METAMORPHOSES OF THE TORYX SHAPE

We will use now the equations for the spacetime properties of a toryx shown in Tables 13.1 and 13.2 to visualize fantastic spacetime transformations of the toryx shape. Figure 13.8 illustrates ten different appearances of a toryx as the steepness angle of a trailing string φ_2 changes from 0^0 to 360^0. These appearances correspond to the change of the relative radius of the leading string b_1 from positive infinity ($+\infty$) to negative infinity ($-\infty$).

Table 13.4. Four principal types of the toryces.

Group	**1**	**2**	**3**	**4**
Reality	*Real*	*Real*	*Imaginary*	*Imaginary*
Sign	(–)	(+)	(+)	(–)
φ_2 range	$0^0 \leftrightarrow 90^0$	$90^0 \leftrightarrow 180^0$	$180^0 \leftrightarrow 270^0$	$270^0 \leftrightarrow 360^0$
b_1 range	$+\infty \leftrightarrow 1$	$1 \leftrightarrow \frac{1}{2}$	$\frac{1}{2} \leftrightarrow 0$	$0 \leftrightarrow -\infty$

Table 13.5. Four main transformations of a toryx.

φ_2	b_1	**Toryx transformation**		**Toryx name**
		from	***To***	
0^0 / 360^0	$\pm\infty$	Imaginary (–)	Real (–)	Negative inversion string
90^0	1	Real (–)	Real (+)	Real inversion string
180^0	$\frac{1}{2}$	Real (+)	Imaginary (+)	Positive inversion string
270^0	0	Imaginary (+)	Imaginary (–)	Imaginary inversion string

Shown in each view with dotted lines are the inversion spheres with the relative radius $b_1 = 1$. We used two criteria for the classification of the toryces. The first criterion is the reality of the translational velocity β_{2t} that can be either *real* or *imaginary*. The second criterion is the sign of the toryx curvature factor q that can be either *positive* or *negative*. Consequently, the toryces are divided into four principle types shown in Table 13.4. The main transformations of a toryx occur at four values of φ_2 and b_1 as shown in Table 13.5.

Real negative toryces ($0^0 \le \varphi_2 \le 90^0$) – When $\varphi_2 = 0^0$, the relative radii b_1 and b_2 of both leading and trailing strings approach positive infinity. Consequently, the trailing string appears as an infinitely long straight line tangential to the inversion sphere. It is called the *negative inversion string*. This toryx has the infinite number of windings w_2; its trailing string propagates at the rotational velocity equal to the ultimate string velocity c, so $\beta_{2r} = 1$, while its translational velocity β_{2t} is equal to zero. Also equal to zero are the frequencies δ_1 and δ_2 of both leading and trailing strings. As φ_2 increases and b_1 decreases, the relative radius of the toryx trailing string b_2 decreases accordingly, making the trailing string to look like a toroidal spiral. At the end of the range, when $\varphi_2 = 90^0$ and $b_1 = 1$, the trailing string disappears and the toryx reduces to a circle called the *real inversion string*.

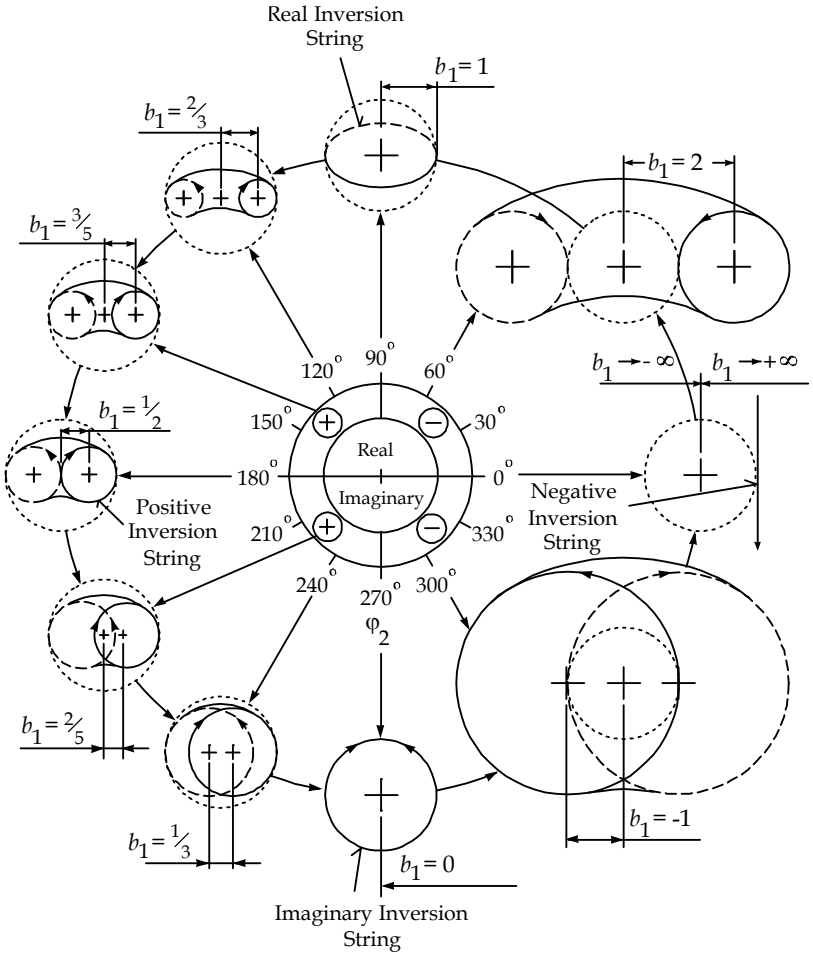

Figure 13.8. Metamorphoses of the toryx shape.

Real positive toryces ($90^0 \le \varphi_2 \le 180^0$) – Within this range, the toryx is still real, but its trailing string is inverted, and its windings are now located inside the inversion sphere. Consequently, the direction of the rotational velocity of the trailing string β_{2r} reverses. As b_1 becomes less than 1, the number of windings w_2 and the absolute value of β_{2r} increase, while the translational velocity β_{2t} decreases. The frequencies of both leading and trailing strings become greater than the frequency f_i, so $\delta_1 > 1$; $\delta_2 > 1$.

At the end of the range, when $\varphi_2 = 180^0$ and $b_1 = ½$, the toryx reduces to a circle with the radius equal to $r_i/2$. It is called the *positive inversion string*. In this toryx the number of windings w_2 approaches infinity. Its trailing string propagates at the rotational velocity equal to the negative ultimate string velocity $-c$ ($\beta_{2r} = -1$), while its translational velocity β_{2t} is

equal to zero. Also equal to zero is the frequency of the leading string δ_1, while the frequency of the trailing string becomes two times greater than the frequency f_i , so $\delta_2 = 2$.

Imaginary positive toryces ($180^0 \leq \varphi_2 \leq 270^0$) – Within this range, the windings of the trailing string overlap each other in a toryx eye like in a so-called *spindle torus*. Its trailing string remains inverted and its windings stay inside the inversion sphere. Therefore, the rotational velocity β_{2r} remains negative and is expressed with a real number. Also expressed with a real number is the frequency δ_2. Several parameters, including w_2, β_{2t}, and δ_1, are expressed with imaginary numbers. Within this range, the rotational velocity β_{2r} and the frequency δ_2 increase with decrease of b_1.

At the very end of the range, when $\varphi_2 \rightarrow 270^0$ and $b_1 \rightarrow 0$, the toryx reduces to a circle with the radius r_i ($b_1 = 1$) called the *imaginary inversion string*. It is located in the plane perpendicular to the plane of the real inversion string. In this toryx, the number of the windings w_2 is equal to zero, both parameters of the trailing string, β_{2r} and δ_2, approach negative infinity, while the two other toryx parameters, β_{2t} and δ_1, approach imaginary positive infinity.

Imaginary negative toryces ($270^0 \leq \varphi_2 \leq 360^0$) – At the very beginning of the range, the toryx appears as the imaginary inversion string that is the same as the imaginary inversion string for the imaginary positive toryces, except that the values of β_{2r}, δ_2, β_{2t} and δ_1 change their signs. Within this range, the windings of the trailing string also overlap one another, but in a different manner than in the imaginary positive toryx. In this toryx, the trailing string becomes outverted, and its windings are now wound outside the inversion sphere. As φ_2 increases, the negative value of b_1 increases; both β_{2r} and δ_2 decrease and their values remain real. Within this range, the values of several other parameters, including w_2, β_{2t}, and δ_1, are expressed with imaginary numbers.

At the end of the range, when $\varphi_2 = 360^0$ and $b_1 \rightarrow -\infty$, the toryx reduces to the same negative inversion string that represents the real negative toryx at $\varphi_2 = 0^0$ and $b_1 \rightarrow +\infty$. Several infinite and zero values of the toryx parameters merge at this point:

Toryx parameters	**Merger of infinities and zeros**	
	$\varphi_2 \rightarrow 0^0$	$\varphi_2 \rightarrow 360^0$
$b_1, b_2, l_1, l_2, \delta_2, t_2$	$+\infty$	$-\infty$
t_1, η_2, w_2	$+\infty$	$+\infty\, i$
$\beta_1, \beta_{1r}, \beta_{2t}, \delta_1,$	$+0$	$+0i$

MATCHED TORYCES

3D-SST considers two types of matched toryces, reality-polarized and charge-polarized. The relative radii of the leading strings of the matched toryces b_1' and b_1'' are related to one another by the equation:

$$b_1'' = \frac{b_1'}{(q_t + 2)b_1' - 1} \tag{13-9}$$

where q_t is the total curvature factor of the matched toryces.

Reality-polarized matched toryces – One of the toryces making up the reality-polarized matched toryces is real, while the other one is imaginary. The total curvature factors q_t of the reality-polarized matched toryces is either negative or positive. Consequently, the reality-polarized matched toryces are divided into two kinds, *negative* and *positive*. For instance, when q_t = -2 and the relative radius of the leading string of one of the toryces b_1' = 2, we find from Equation (13-9) that for the other toryx b_1'' = -2.

Charge-polarized matched toryces – In one of the toryces making up the charge-polarized matched toryces the curvature factor q is positive, while in the other one it is negative. Both toryces that constitute the charge-polarized matched toryces are either real or imaginary. Consequently, the charge-polarized matched toryces are divided into two kinds, *real* and *imaginary*. For instance, when q_t = 0 and the relative radius of the leading string of one of the toryces b_1' = 2, we find from Equation (13-9) that for the other toryx b_1'' = ⅔.

CONSTRUCTION OF HELYX

Similarly to the toryx, the helyx is a double-level helicola. In the helyx, the first level of the helicola is made of one double-helical spiral (Fig. 13.9). There is an easy way to visualize the double-helical spiral. Consider two points, *a* and *b*, rotating around a pivot point *m* with the rotational velocity $\tilde{V}_{1r}$, while the pivot point *m* propagates along a straight line O_1O_1 with the translational velocity $\tilde{V}_{1t}$. Each point, *a* and *b*, leaves a helical spiral trace A_1 winding around the straight line O_1O_1. The two traces A_1 are separated from each other by 180 degrees and form a double helix called the *helyx leading string*.

The second level of the helyx is made of two double helices, each wrapped around one of the helical spirals of the leading string. The two double helices of the second level of the helyx form the *helyx trailing string*. For the sake of simplicity, Figure 13.10 shows a helyx with only one double-helical spiral of the leading string. There the leading string is represented by a helical trace A_1 that is accompanied by two helical traces A_2 representing the trailing string.

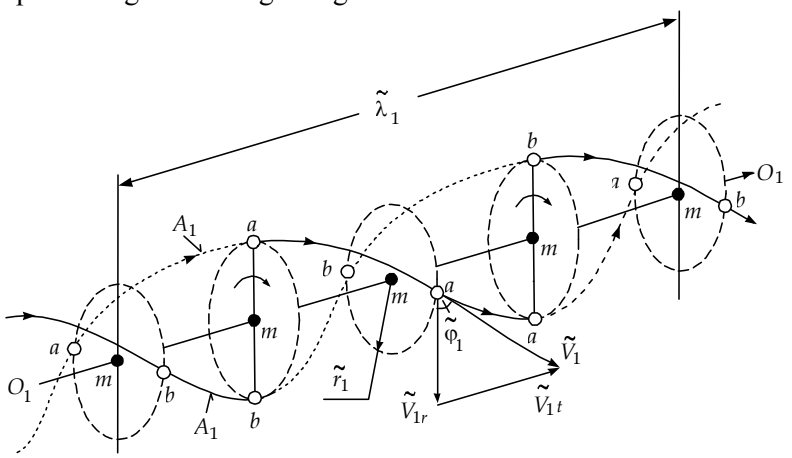

Figure 13.9. The leading string of a helyx.

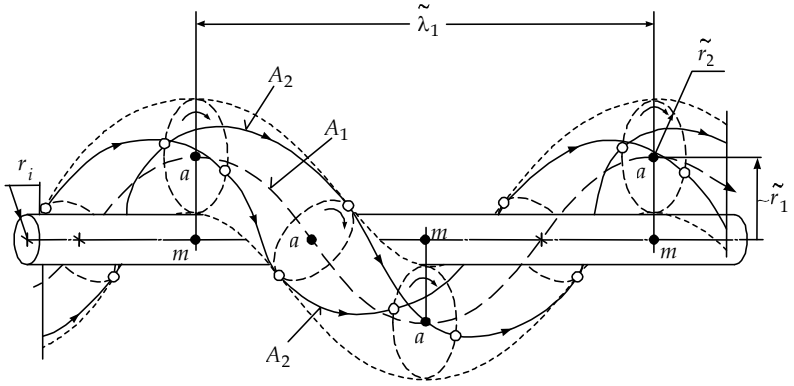

Figure 13.10. Construction of one of two double-helical leading strings.

In spite of many features common for both the helyx and the toryx, the helyx is different than the toryx in several ways. First of all, unlike the double-circular leading string of the toryx, the leading string of the helyx is double-helical. Secondly, the steepness angle of the helyx trailing strings $\tilde{\varphi}_2$ is much greater than the steepness angle φ_2 of the toryx.

Also different are the magnitudes and realities of both rotational and translational velocities of the trailing strings. In the toryx, the rotational velocity V_{2r} is always real; it can vary from negative to positive infinity, while the translational velocity V_{2t} can be either real or imaginary. Conversely, in the helyx, the translational velocity $\tilde{V}_{2t}$ is always real and can vary from negative to positive infinity, while the rotational velocity $\tilde{V}_{2r}$ can be either real or imaginary.

SPACETIME PARAMETERS OF HELYX

In the diagrams shown in Figure 13.11 the spacetime parameters of leading and trailing strings form the sides of right triangles. Therefore, we can readily establish the relationships between these parameters by using the Pythagorean Theorem. Helical trailing strings of the helyx propagate along their helical paths in synchrony with helical leading strings, so, the translational velocity of the trailing string $\tilde{V}_{2t}$ is equal to the spiral velocity of the leading string $\tilde{V}_1$.

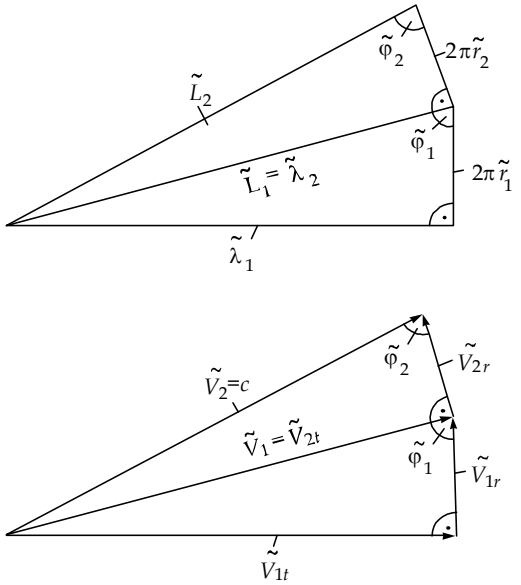

Figure 13.11. Spacetime parameters of a helyx.

The spacetime properties of the helyx are governed by four fundamental equations shown in Table 13.6. One can clearly see some similarity between the fundamental spacetime equations for the helyx (Table 13.6) and the toryx (Table 13.1). Equations for the radius of the real inversion string r_i of the toryx and the helyx are identical. For the helyx,

the ratio of radii of trailing and the leading strings $\tilde{r}_2$ and $\tilde{r}_1$ is equal to the *sine* of the steepness angle, rather than to the *cosine* of this angle used for the toryx. Similarly to the toryx, the spiral velocity of the helyx trailing string $\tilde{V}_2$ is equal to the ultimate string velocity *c*. Adding to the similarities between the helyx and the toryx is the fact that for both of them the radius r_i and the frequency f_i are respectively expressed by the same equations.

Table 13.6. Fundamental spacetime equations for a helyx.

Parameter	Equation	
Radius of real inversion string	$r_i = \tilde{r}_1 - \tilde{r}_2 = const.$	(13-10)
Length of one winding of trailing string	$\tilde{\lambda}_2 = \tilde{L}_1$	(13-11)
The steepness angle of trailing string	$\sin\tilde{\varphi}_2 = \frac{\tilde{r}_2}{\tilde{r}_1}$	(13-12)
The spiral velocity of trailing string.	$\tilde{V}_2 = \sqrt{\tilde{V}_{1t}^2 + \tilde{V}_{1r}^2 + \tilde{V}_{2r}^2} = c$	(13-13)

As we have done in application to the toryx, we can take advantage of the constancy of the radius r_i, the ultimate string velocity *c*, and the frequency f_i to express the spacetime parameters of a helyx in relative terms. This will make these parameters dimensionless, drastically simplifying the mathematical model. With these simplifications, we can readily derive the equations for the helyx spacetime parameters as a function of the relative radii of their leading string $\tilde{b}_1$ shown in Table 13.7.

The helyx curvature factor $\tilde{q}$ is assumed to be equal to:

$$\tilde{q} = -\sqrt{1 - \left(\frac{\tilde{r}_2}{\tilde{r}_1}\right)^2} \qquad (13\text{-}14)$$

Both the toryces and the helyces have their respective counterparts, the *antitoryces* and the *antihelyces*. The trailing strings in the antitoryces and the antihelyces are turned inside out in respect to their states in the respective toryces and helyces.

Table 13.7. Spacetime parameters of a helyx for a middle point.

Leading string	Trailing string
$\widetilde{b}_1 = \dfrac{\widetilde{r}_1}{r_i}$	$\widetilde{b}_2 = \dfrac{\widetilde{r}_2}{r_i} = \widetilde{b}_1 - 1$
$\cos\widetilde{\varphi}_1 = \dfrac{\widetilde{b}_1\sqrt{(2\widetilde{b}_1 - 1)}}{(\widetilde{b}_1 - 1)^2}$	$\sin\widetilde{\varphi}_2 = \dfrac{\widetilde{b}_1 - 1}{\widetilde{b}_1}$
$\widetilde{\eta}_1 = \dfrac{\widetilde{\lambda}_1}{2\pi r_i} = \sqrt{\dfrac{(\widetilde{b}_1 - 1)^4 - \widetilde{b}_1^2(2\widetilde{b}_1 - 1)}{2\widetilde{b}_1 - 1}}$	$\widetilde{\eta}_2 = \dfrac{\widetilde{\lambda}_2}{2\pi r_i} = \dfrac{(\widetilde{b}_1 - 1)^2}{\sqrt{2\widetilde{b}_1 - 1}}$
$\widetilde{l}_1 = \dfrac{\widetilde{L}_1}{2\pi r_i} = \dfrac{(\widetilde{b}_1 - 1)^2}{\sqrt{2\widetilde{b}_1 - 1}}$	$\widetilde{l}_2 = \dfrac{\widetilde{L}_2}{2\pi r_i} = \dfrac{\widetilde{b}_1(\widetilde{b}_1 - 1)}{\sqrt{2\widetilde{b}_1 - 1}}$
$\widetilde{w}_1 = 1$	$\widetilde{w}_2 = 1$
$\widetilde{\beta}_{1t} = \dfrac{\widetilde{V}_{1t}}{c} = \dfrac{\sqrt{(\widetilde{b}_1 - 1)^4 - \widetilde{b}_1^2(2\widetilde{b}_1 - 1)}}{\widetilde{b}_1(\widetilde{b}_1 - 1)}$	$\widetilde{\beta}_{2t} = \dfrac{\widetilde{V}_{2t}}{c} = \dfrac{\widetilde{b}_1 - 1}{\widetilde{b}_1}$
$\widetilde{\beta}_{1r} = \dfrac{\widetilde{V}_{1r}}{c} = \dfrac{\sqrt{2\widetilde{b}_1 - 1}}{\widetilde{b}_1 - 1}$	$\widetilde{\beta}_{2r} = \dfrac{\widetilde{V}_{2r}}{c} = \dfrac{\sqrt{2\widetilde{b}_1 - 1}}{\widetilde{b}_1}$
$\widetilde{\beta}_1 = \dfrac{\widetilde{V}_1}{c} = \dfrac{\widetilde{b}_1 - 1}{\widetilde{b}_1}$	$\widetilde{\beta}_2 = \dfrac{\widetilde{V}_2}{c} = 1$
$\widetilde{\delta}_1 = \dfrac{\widetilde{f}_1}{f_i} = \dfrac{\sqrt{2\widetilde{b}_1 - 1}}{\widetilde{b}_1(\widetilde{b}_1 - 1)}$	$\widetilde{\delta}_2 = \dfrac{\widetilde{f}_2}{f_i} = \dfrac{\sqrt{2\widetilde{b}_1 - 1}}{\widetilde{b}_1(\widetilde{b}_1 - 1)}$

A Connection With A Physical World

It took me almost twelve years to derive the mathematical model of the toryx and the helyx in the form described in this chapter. The model excited me because of simplicity of its fundamental equations and also by the beauty and sophistication of produced spacetime shapes of the toryx and the helyx. But, as an applied research worker by trade, I could not stop myself from thinking about a possible application of the developed mathematical model to a physical world.

Several results produced by the model were almost screaming to tell me that they reflect the laws of nature. The most obvious among these results was the relationship between the radius of the toryx leading string r_1 and the translational velocity of the trailing string V_{2t}. According to 3D-SST, this relationship is given by the equation:

$$V_{2t} = c\frac{\sqrt{2r_1 / r_i - 1}}{r_1 / r_i} \tag{13-15}$$

For the case, when the radius of the toryx leading string r_1 is much greater than the radius of the real inversion string r_i, Equation (13-15) reduces to the form:

$$V_{2t} = c\sqrt{\frac{2r_i}{r_1}} \tag{13-16}$$

But, since both the ultimate string velocity c and the radius r_i are constant, the last equation tells us that the translational velocity V_{2t} is related to the radius r_1 in accordance with the well-known inverse-square law. Bingo! According to 3D-SST, Equation (13-16) is applicable to an atomic structure if the inversion radius r_i is equal to:

$$r_i = \frac{Ze_0^2}{8\pi\varepsilon_0 m_0 c^2} \tag{13-17}$$

where: m_0 = electron rest mass
e_0 = elementary charge
ε_0 = electric constant
Z = atomic number.

The same Equation (13-16) is applicable to a planetary system if the inversion radius r_i is equal to:

$$r_i = r_j = \frac{mG}{2c^2} \tag{13-18}$$

where: m = rest mass of a star
G = Newtonian constant of gravitation.

Another strong indication of a natural character of the toryx is its ability to be either right-handed or left-handed. This is similar to a spin of an electron, also to the rotation of the planets around their axes. But what impressed me the most was the ability of the toryx to be turned inside out. This type of transformation could be associated with the creation of opposite electric charges. Also, after recollecting Einstein's general theory of relativity, I thought that the toryx gravitational mass could be dependent on its curvature.

All these associations of the toryx with nature forced me to ask myself a daring question if it is possible to relate the spacetime properties of the toryx to its physical properties. I wanted to know the same thing about helyx. Similarly to the atomic electrons, the toryces could be at

various quantum energy states, and emit the helyces when their quantum energy states were reduced. Consequently, the toryces could serve as the building blocks for the creation of the mass elementary particles, while the helyces could form the radiation elementary particles.

I felt excited about a possible practical application of a pure abstract mathematical model to a real world. At the same time, I was fully aware that this venture will move my research from a safe heaven of mathematics based on prudent assumptions and synonymously verifiable results, into a less defined paradigm of physics and inevitably controversial propositions. Well, there was a very strong reason why, in spite of my full understanding of the potential obstacles, I still decided to go ahead with the project: I tried to stop doing it many times, but a strong desire to see some practical results eventually prevailed.